Available online at www.sciencedirect.com

ScienceDirect

Energy Procedia 114 (2017) 2467 – 2480

Energy Procedia

13th International Conference on Greenhouse Gas Control Technologies, GHGT-13, 14-18 November 2016, Lausanne, Switzerland

A new multi-bed vacuum swing adsorption cycle for CO_2 capture from flue gas streams

Paul A. Webley[a,b,c]*, Abdul Qader[b], Augustine Ntiamoah[a], Jianghua Ling[a,d], Penny Xiao[a], Yuchun Zhai[d]

[a]*The University of Melbourne, Department of Chemical and Biomolecular Engineering*
[b]*CO2CRC Limited*
[c]*The Peter Cook Centre for Carbon Capture and Storage*
[d]*School of Material and Metallurgy, Northeastern University, Shenyang, Liaoning 110004, PR China.*

Abstract

Adsorption Processes for CO_2 capture have been extensively researched within the last decade and have been piloted at many field installations and in research laboratories. Many reported VSA cycle designs for CO_2 capture are based on single- and dual-adsorbent beds. The performance of such cycles is typically poor due to the lack of room to incorporate more relevant auxiliary intermediate process steps such as pressure equalization, co-current purge, etc. Very low vacuum pressures (< 3kPa) are therefore necessary to achieve higher CO2 purity. This is difficult and expensive to provide at large scale. To address this concern, a new 4-bed PVSA cycle has been developed in our laboratory and tested experimentally and through simulation. The cycle configuration provides a means to internally recycle parts of the product and CO_2-lean gases to enhance the separation efficiency and also to minimize energy consumption. A dry gas mixture of 15%CO2 in N_2 was used as the feed gas and zeolite 13x as the adsorbent. A product purity of 92.4% was obtained at 64% recovery at 8 kPa desorption, while 5 kPa desorption produced >75% recovery with a purity of > 95%CO_2. The calculated specific power consumption is approximately 0.33 MJ/kgCO_2. Including two pressure equalization steps after a product rinse step contributed to the relatively lower specific power consumption achieved.

Peer-review under responsibility of the organizing committee of GHGT-13.

Keywords: adsorption, vacuum swing adsorption, CO2 capture

* Corresponding author. Tel.: +61-3-90357873; fax: +0-000-000-0000 .
E-mail address: paul.webley@unimelb.edu.au

Peer-review under responsibility of the organizing committee of GHGT-13.
doi:10.1016/j.egypro.2017.03.1398

1. Introduction

Pressure and Vacuum Swing Adsorption (VSA) technology has been widely studied for post-combustion CO_2 capture at both laboratory and pilot scale levels in the quest for alternative more environment-friendly and cost-effective CO_2 capture techniques [1,2]. Consequently, a variety of process configurations have been investigated, which differ by the type of adsorbent, distinct cycle steps and their sequence, operating conditions (temperature, pressure, flow velocity, etc) and cycle step times. Improvements continue to be sought, in both adsorbents and process cycles to further reduce energy consumption and also to enable the use of moderate regeneration conditions that can be easily achieved on a large scale.

Many reported VSA cycle designs for CO_2 capture are based on single- and dual- adsorbent beds [3,4]. The performance of such cycles is typically poor due to the difficulty of accommodating more relevant auxiliary intermediate process steps [5]. Very low vacuum pressures (< 3kPa) are invariably used in such designs to achieve better separation performance. For example, Shen et al [6] reported a study based on a single-bed VSA cycle with activated carbon as the adsorbent. The cycle sequence included feed pressurization, adsorption, evacuation and light reflux. The cycle yielded a modest performance of 53.8% product purity, 66% recovery and a productivity of 1.59 mol/kg/hr under operating pressures of 131.3 and 5 kPa for adsorption and desorption pressures, respectively. With a lower evacuation pressure of about 3 kPa, Haghpanah et al [7] obtained an optimized performance of 90% purity-recovery of CO_2 product from a synthesized flue gas with CO_2 concentration of 15% using a simple four-step cycle including light product pressurization (LPP). An energy consumption of 131 kWh/ton CO_2 (0.47 MJ/kgCO_2) and productivity of 0.57 mol CO_2/m^3 adsorbent were also calculated. Farooq and co-workers [8] performed an experimental pilot-scale study based on a 2-bed/6-step process cycle with zeolite 13x as the adsorbent. The cycle sequence included pressurization with light product (LPP), idle, adsorption, co-current blowdown (which was aided by a vacuum pump), and counter-current evacuation. A very low vacuum pressure of 2 kPa was used to obtain a higher purity of 94.8% and a recovery of 89.7% CO_2. The measured specific power consumption was very high >470 kWh/ton CO_2 (1.7 MJ/kgCO_2).

The most common approach used to achieve high CO_2 product purity is to purge the bed with some of the CO_2 product, which mimics the reflux operation in distillation systems. The main idea of adding this heavy reflux (HR) step is to enrich the feed end with CO_2 by displacing the lighter component prior to the evacuation step [9–12]. However, while enhancing product purity, the purge step may add to power consumption of the process if the purge gas is compressed before feeding to the bed. Intermediate pressure equalization (PE) is also widely used in multi-bed adsorption cycles. In addition to saving the mechanical energy in the high pressure bed [13], PE also helps to further advance the CO_2 front prior to desorption and enrich the gas phase in CO_2 by dropping the pressure and transferring void space gas from the top of the bed to another bed to repressurize the latter [10]. A previous experimental study in our group [12] using three adsorbent beds and a nine-step cycle including PE, HR and (LPP) produced a high purity of 95.2% CO_2 and recovery of 70% with specific power consumption of 12.1 kW/TPDc (1.05 MJ/kgCO_2) at a desorption pressure of 5 kPa. A U.S. patent [14], assigned to Air Liquide Advanced Technologies U.S. LLC presents a VSA process with a high pressure product rinse step for CO_2 capture from low-concentration sources. Simulations in Aspen Adsorption of a 4-bed/8-step VSA cycle with zeolite 13x adsorbent yielded 82.8 % product purity and 89.2 % recovery at a power consumption of 8.01 kW/(t/d) (0.7 MJ/kgCO_2). A pilot scale experimental study by Wang et al [26] (2013) used a low but more realistic vacuum pressure of 7-8 kPa and employed the PE, HR and light reflux (LR) steps in a 3bed/8step VPSA cycle on zeolite 13x. Higher recoveries in the range of 85-95% CO_2 were obtained, but purity was limited to 82% CO_2. The measured specific power consumption was also very high (1.79 – 2.14 MJ/kgCO_2). The LR step is widely used in hydrogen PSA and oxygen cycles (stripping cycles); however, this needs careful control when applied in CO_2 PSA/VSA cycles. As more purge gas is admitted to increase recovery, product purity decreases rapidly as nitrogen breaks through quickly into the product stream due to the dispersive nature of the purge wave exacerbated by the strongly non-linear and favorable isotherm shape for CO_2 on the adsorbent, relative to nitrogen [12]. Addition of the LR gas can also easily produce a product flow higher than the evacuation rate prior to commencing the purge step, which can also lead to more power consumption by the vacuum pump due to the increased flowrate, which could outweigh the gains in recovery.

Most current reports show that deep vacuum levels (<5 kPa) are essential for the CO2VSA process to achieve CO_2 purities of over 90% with recovery ranging from 70% to 90% [7,8,12,16–18]. It is still considered difficult to achieve both high CO_2 purity and recovery by a single stage VSA process without deep vacuum desorption, or resorting to dual reflux cycles. A study by Zhang et al [12] found that optimal performance based on zeolite 13x (in terms of purity, recovery and specific power) occurred at 3 kPa evacuation pressure. The main issue of concern is the practicality of achieving such a low vacuum level at large scale in a cost effective way. Vacuum pump efficiency decreases with decreasing vacuum level, and there is a wide disparity between measured and calculated power consumption at vacuum levels below 5 kPa [8]. The deeper vacuum will also require multistage pump units which would increase both capital and operating costs. In addition, the operating valves which can seal at low pressures are very large and expensive [19]. Two-stage VSA processes have been proposed, where the operating conditions are manipulated to obtain very high recovery but lower purity in the first stage of processing, and the entire product is fed to a second unit to further concentrate the CO_2. For example, Wang et al. [20] studied a two-stage VSA process for CO_2 capture at a desorption pressure of 10 kPa. In their experiments, an overall CO_2 product with a purity of 96.5% and a recovery of 93.4% was obtained but with a corresponding increase in capital and operating cost for the extra VSA unit. Multi-bed cycle designs, incorporating more intermediate steps as often used in conventional hydrogen PSA systems may help achieve further gains in the separation performance of CO2VSA units without the need for a second VSA unit. Such designs form the subject of this study.

Trade-offs invariably exists in the performance of PSA systems. It is therefore unlikely that any design choice for exploiting the adsorbent properties for a particular feed gas condition will be optimal for all performance variables. In this study, we focused on achieving higher product purity and lower specific power consumption for carbon capture and storage (CCS) applications as higher product purity reduces the costs of further processing of the product gas for geological storage. This goal implies that we must ensure that most of the void space and co-adsorbed nitrogen gas ahead of the CO_2 front in the column after adsorption is removed before beginning product recovery. To this end, we proposed a new VSA process cycle that employs a heavy product purge which is carried out after a pressure equalization step (when the bed pressure at this stage is less than atmospheric hence avoiding the need for a purge recycle compressor), followed by two more pressure equalization steps prior to desorption. As a consequence, most void space gases are removed and a considerable reduction in the column pressure is also achieved before desorption, which in turn leads to enhanced product purity and a reduction in the amount of work performed by the vacuum pump. Any CO_2 in the rinsing effluent is recovered by using it to directly repressurize another bed at a lower pressure. The performance of the cycle sequence is evaluated using an experimental 4-bed VSA apparatus and a zeolite 13x adsorbent.

Nomenclature

HR	Heavy Reflux
LPP	Light Product Pressurisation
LR	Light Reflux
PE	Pressure Equalisation
PSA	Pressure Swing Adsorption
SCADA	Supervisory, Control And Data Acquisition
VSA	Vacuum Swing Adsorption

2. Experimental Program

Both experimental and simulation work was conducted to test our new process cycles and to help interpret and understand the data obtained.

2.1. CO_2 Capture Adsorbent

The adsorbent used in this study is a commercial zeolite 13x (PSAO2HP- manufactured by UOP), which was chosen based on its relatively higher differential CO_2 loading, CO_2/N_2 selectivity, and superior performance in previous CO2VSA studies [21,22,23]. Dry premixed gas of 15% CO_2 in N_2 was used as feed gas – this is representative of flue gas composition. Pure component isotherms of CO_2 and N_2 on the adsorbent were measured using a volumetric apparatus, the Micromeritics ASAP2010, at temperatures of 0, 30 and 60 °C, over a pressure range from 0 to 113 kPa. Adsorbents were degassed at < 10^{-4} torr at 400°C overnight. The isotherm data are shown in Fig. 1. The isotherms were very well described by the Dual Site Langmuir model. The model equation and fitted parameters are given in equation 1 and Table 1 respectively, where we have deliberately used the version as encoded in Aspen Adsorption for ease of use by the reader. Zero loading heats of adsorption values were calculated from the fitted isotherm model by using the Clausius-Clayperon equation to be -35 kJ/mol and -16 kJ/mol for CO_2 and N_2 respectively.

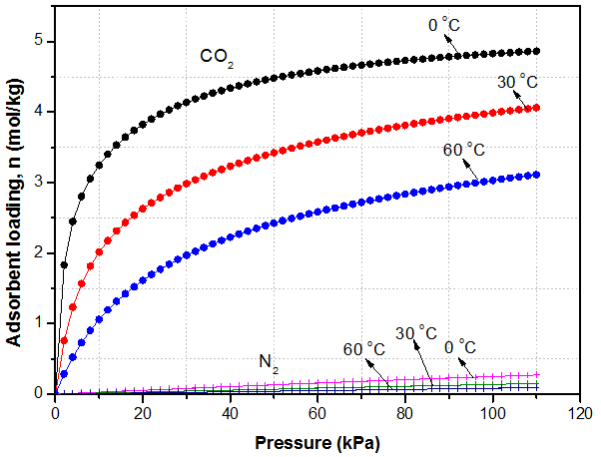

Fig. 1. Adsorption isotherms for CO_2 and N_2 on zeolite 13X at 0, 30 and 60°C.

$$n_i = \frac{IP_{1i} \times exp\left(\frac{IP_{2i}}{T}\right) \times P_i}{1 + IP_{3i} \times exp\left(\frac{IP_{4i}}{T}\right) \times P_i} + \frac{IP_{5i} \times exp\left(\frac{IP_{6i}}{T}\right) \times P_i}{1 + IP_{7i} \times exp\left(\frac{IP_{8i}}{T}\right) \times P_i} \quad (1)$$

Where n_i is the equilibrium loading of component i (kmol/kg-adsorbent), P_i is equilibrium pressure of component i (bar) and T is temperature (K). Units of the isotherm parameters are derived as IP1 = kmol.kg-1.bar-1; IP2 = K; IP3 = bar-1; IP4 = K; IP5 = kmol.kg-1.bar-1; IP6 = K; IP7 = bar-1 and IP8 = K. Mixed gas data were represented by the Extended Langmuir Model.

Table 1. Dual-site Langmuir adsorption equilibrium parameters of CO_2 and N_2 on UOP PSAO2HP zeolite 13X at temperatures of 0, 30 and 60°C and pressures of 0 – 1.1 bar.

Component	IP1	IP2	IP3	IP4	IP5	IP6	IP7	IP8
CO_2	1.82E-08	5302.4	3.18E-05	4809.2	2.71E-07	3349.5	3.85E-05	3684.8
N_2	3.80E-07	2066.9	0.017	0	0	0.549	0.776	4.16

2.2. Experimental Apparatus

The experimental VSA apparatus used is shown in Fig. 2. The system consists of four adsorber columns (stainless steel) of internal diameter 2.0 cm and packing length 90.0 cm. Each column was packed with 195 g of the adsorbent. Prior to packing in the columns, the material was activated by heating to a temperature of 350°C in a furnace overnight,

and then cooled under a flow of nitrogen gas. Control valves (Samsons), and flow meters (Yokogawa) are installed on the feed, purge, waste and product lines to deliver and maintain the designed pressures and flowrates, while pressure equalization and waste recycle rates are controlled by needle valves. A number of pressure transducers and thermocouples (T-type) are fitted to monitor stream and bed pressures and temperatures during operation. In addition to a feed tank, intermediate product and waste storage tanks are also provided from which gases can be recycled to the columns when required by the cycle design. A rotary vane vacuum pump (KSV-65) is used for evacuation while a compressor (Thomas) is installed on the product purge line. During the runs, gas samples are continuously taken from both product and vent lines for analysis on a CO_2 composition analyzer (Servomex). The apparatus is operated from a computer through a Citect-SCADA/GE-FANUC controller interface. Cycle operation is entirely automated and realized by switching on/off pneumatically-actuated solenoid valves to change the direction of gas flow for the different steps of the cycle according to a programmed PLC logic.

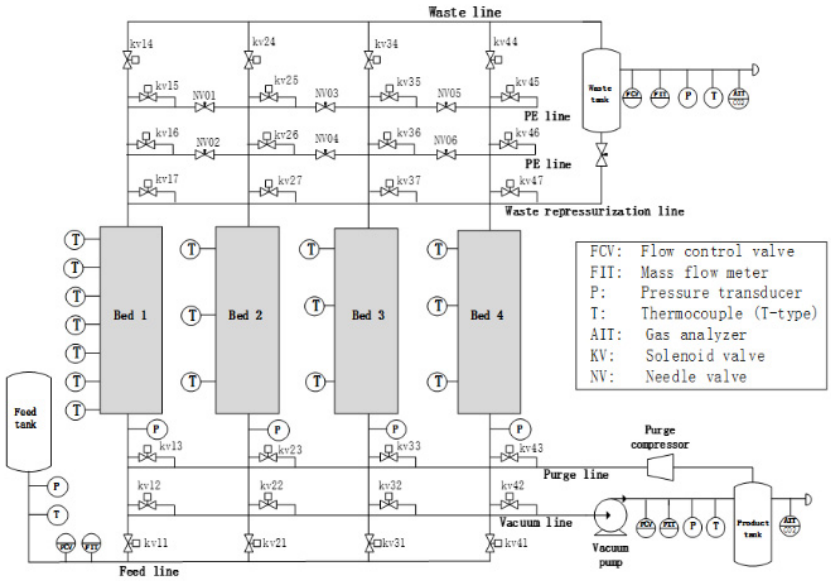

Fig. 2. Simplified schematic diagram of the 4-bed PSA/VSA experimental system

2.3. Cycle Design and Operating Procedure

The sequence of steps used is as follows: I. Adsorption; II. Provide pressure equalization 1; III. Product rinse + supply to repressurization; IV. Provide pressure equalization 2; V. Provide pressure equalization 3; VI. Evacuation; Receive pressure equalization 3; VII. Receive pressure equalization 2; VIII. Receive pressure equalization 1; and IX. Repressurization. The sequence is illustrated in Figs. 3a and b for one and four beds respectively.

The pressure equalization step preceding the product rinse/purge step was included to lower the column pressure to a sub-atmospheric level such that the purge gas can be fed to the column without compressing it. Generally, the amount of purge gas used should be based on the level of purity required. However, because the purge step is coupled with a repressurization step, the amount of purge gas (or the step duration) is then dependent on when the pressure in the coupled bed reached atmospheric, and hence this factor could be influenced by the first PE pressure of the bed. The subsequent two pressure equalization steps are essential in further advancing the CO_2 front in the column by removing more gas from the top of the bed which has higher N_2 composition.

a

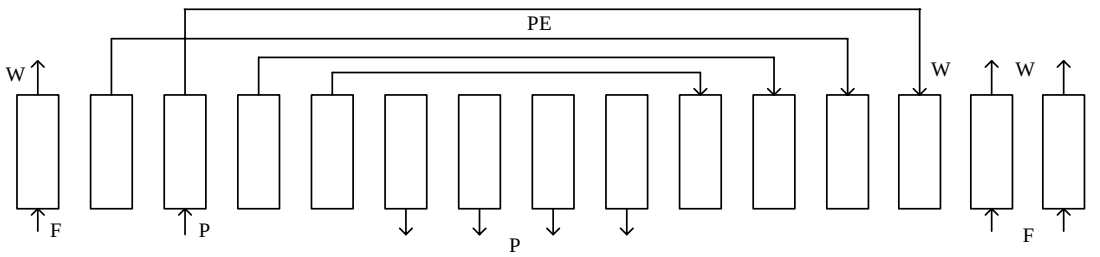

b

B1	F	PE	RN	PE	PE	EV			PE	ID		PE	ID		PE	Rp	F			
B2	ID	PE	Rp	F			PE	RN	PE	PE	EV			PE	ID			PE	ID	
B3	EV				PE	ID			PE	ID		PE	Rp	F			PE	RN	PE	PE
B4	ID			PE	ID		PE	Rp	F			PE	RN	PE	PE	EV				PE
t(s)	60	10	10	10	10	60	10	10	10	10	60	10	10	10	10	60	10	10	10	10

Fig. 3- VSA cycle sequence and operating schedule for four adsorbent bed system. Step times are shown for a cycle run with a total of 80 seconds for adsorption.
F = Feed (adsorption); PPE = provide pressure equalization; EV = Evacuation (desorption); RPE = Receive pressure equalization; FP = Repressurization by feed gas; RN = CO_2 product rinse; ID = idle.

Moreover, the two PE steps lower the column pressure before desorption, and thus enrich the vapor phase in CO_2 prior to pump down. In addition, the PE steps reduces the mechanical work performed by the vacuum pump. This avoids the need for additional vacuum pump at the light-product end of the column to maintain the column pressure at the intermediate level [7]. With the product rinse effluent recycled, the only point of loss of CO_2 is through the effluent of the feed step; hence, recovery can be controlled by manipulating the breakthrough of CO_2 during adsorption. PSA/VSA cycle design is bound by scheduling constraints, and more adsorbent beds are usually required when several steps are involved with couplings among the beds as in this case. In this experiment, we focused on the effects of cyclic design and operation parameters on the processing performance, so continuous feeding was not employed. With the available experimental system (consisting of 4 adsorber columns), utilizing the nine distinct cycle steps in their preferred sequence results in 20 unit steps as illustrated in Fig. 3b. As can be seen, there is discontinuity in feeding and some idle steps are also included to synchronize cycle timing.

The experiments were conducted at room temperature (20± 3°C). In all the runs, adsorption pressure and feed flowrate were kept constant at 1.1 bar.a and 5.0 SLPM respectively. This corresponds to a bed velocity of 0.4 cm/s on the feed step and 90 cm/s at the start of the vacuum step. The durations of the pressure equalization and product rinse steps were also kept constant at 10 s (which were found to be adequate for all the cases studied). The parameters which were deliberately varied to assess their effects are the adsorption step duration and vacuum pressure. The adsorption time was varied from 40 to 120s which directly controls the extent of CO_2 breakthrough and hence the CO_2 recovery and eventual purity. The duration of the desorption (evacuation) step also changed with the change of adsorption time according to the cycle schedule, giving total cycle times ranging from 240 to 560 s although in each case the vacuum valve setting was adjusted to maintain the desired end of step vacuum pressure. The operating conditions are summarized in Table 2. The desired stream flowrate and pressure levels were achieved by manipulating the percentage opening of the flow control valves. Since the effluent of the product rinse step was recycled, it can be considered an internal recycle process and therefore its effect is not discussed here.

Table 2. Operating conditions and step times for various cycle runs

Run	Adsorption pressure, kPa	Desorption pressure, kPa	Feed flowrates Litre/min	Step times				
				t_{RN} (s)	t_{Rp} (s)	$t_{F\ (total)}$ (s)	t_{PE} (s)	$^{*}t_{EV\ (total)}$ (s)
1	110	8	5.0	10	10	40	10	50
2	110	8	5.0	10	10	60	10	70
3	110	8	5.0	10	10	80	10	90
4	110	8	5.0	10	10	100	10	110
5	110	8	5.0	10	10	120	10	130
6	110	5	5.0	10	10	40	10	50
7	110	5	5.0	10	10	60	10	70
8	110	5	5.0	10	10	80	10	90
9	110	5	5.0	10	10	100	10	110
10	110	5	5.0	10	10	120	10	130

$^{*}t_{EV\ (total)} = t_{F\ (total)} + t_{PE}$

3. Simulation: Aspen Adsorption

The commercial Aspen adsorption simulator was used to simulate the process cycle for the purposes of interpreting the experimental data and to extend the range of the data. A non-isothermal model was utilized and the dual-site Langmuir model -DSL (equation 1), the linear driving force model and Ergun equation were used to represent the adsorption equilibrium, mass transfer rate and pressure drop across the bed respectively. Mixed-gas adsorption equilibrium models are ideally preferred for more effective process simulations, and are commonly predicted based on pure component isotherms using the ideal adsorbed solution theory (IAS) or competitive Langmuir models [25]. However, since the simulation tool does not show how the pure component parameters can be used to obtain the mixed-gas component model parameters, as also noted by Ritter et al [27], the DSL model was used in the simulations. Ritter et al [27,28], showed that fits to the DSL model matched several mixed-gas adsorption equilibrium data sets very well. The column/bed characteristics provided as inputs to the model are presented in Table 3.

The model equations were solved using the numerical method of lines, and 90 nodes were used to discretize the spatial domain by using the first order upwind differencing scheme (UDS1). One bed is used to simulate the four-bed process. For bed interactions (e.g. pressure equalization), temporal effluent arrays (flow, pressure, composition and temperature) from the depressurizing step were retained and later used when the bed underwent a pressurizing pressure equalization step.

Table 3. Adsorbent and Bed Properties

Parameter	Value	Parameter	Value
Length(m)	0.90	Pellet diameter(mm)	2.0
Internal Bed Diameter (m)	0.020	Bed Specific Heat Capacity kJ/kg.K)	1.0
Wall thickness (cm)	0.3	Linear driving force constant, CO_2 (s^{-1})	0.5
Packing density (kg/m^3)	689.3	Linear driving force constant, N_2 (s^{-1})	0.3
Inter-particle voidage	0.35	Pellet diameter(mm)	2.0
Intra-particle voidage	0.60		

4. Results and Discussion

4.1. Column Temperature and Pressure Histories

The transient profiles of pressure, temperature and concentration are very important in understanding the final performance of PSA experiments. Fig. 4 shows the pressure history of the first column during the last cycle after cyclic steady state has been attained for a representative run 3 (see Table 2).

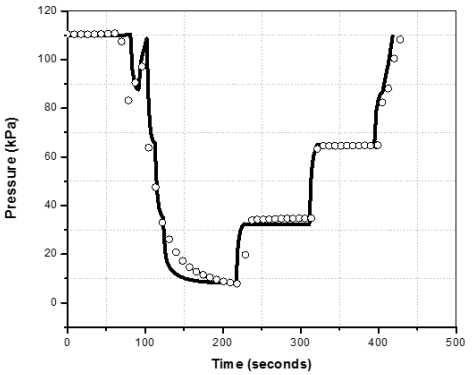

Fig. 5 shows the temperature variations at three locations in the bed (10, 20 and 40 cm) with respect to cycle time for the same run. There were no significant temperature swings in the thermocouples located on the upper part of the bed, which indicate that CO_2 adsorption and desorption were primarily confined to the first half of the bed for this particular run. After adsorption, the temperature in the bed up to 10 cm from the feed end rose from 23 to 31°C. After the rinse step the temperature has significantly increased to 41°C which indicates adsorption of more CO_2 (i.e. the CO_2-rich product with higher heat of adsorption displacing co-adsorbed N_2 in the bed). The temperature then decreased to 36°C with the following PE steps which are actually a desorption step and therefore endothermic, with further decrease during the evacuation step to about 22°C as more CO_2 is recovered from the bed. The predicted pressure- and temperature- time histories were generally in good agreement with the profiles measured with the experimental system as seen in the Fig 4 and 5.

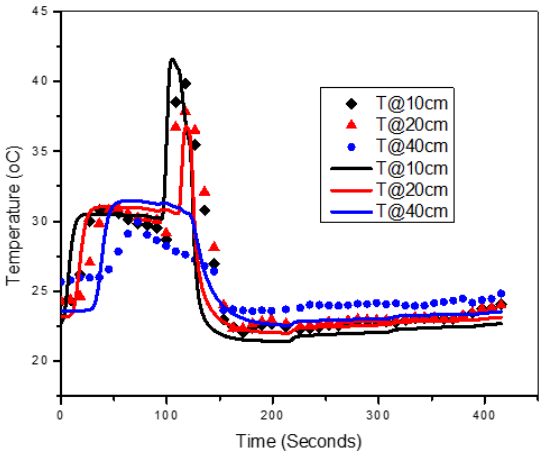

Fig. 5 Example temperature profile at three locations within the bed for a complete cycle at cyclic steady state. (Run 3, Table 2). Symbol = experiments, line = simulation.

4.2. Cycle Performance

Summarized performance results in terms of product purity, recovery, specific power consumption and adsorbent productivity are presented in Table 4 for the experimental runs. In Fig. 6, product recovery is plotted against purity for both experimental and predicted results at the different vacuum pressures to show the agreement between the two. The specific energy consumption was calculated using the adiabatic power equation (equation 2).

$$\text{Energy (kJ)} = \sum_{i=1}^{i=n} \frac{k}{k-1} \frac{Q_{feed} P_{feed}}{\eta} \left[\left(\frac{P_{feed}}{P_{atm}} \right)^{\frac{k-1}{k}} - 1 \right] \Delta t + \sum_{i=1}^{i=n} \frac{k}{k-1} \frac{Q_{vac} P_{vac}}{\eta} \left[\left(\frac{P_{atm}}{P_{vac}} \right)^{\frac{k-1}{k}} - 1 \right] \Delta t \qquad (2)$$

where Q is volumetric flow rate (m^3/s), and P is pressure. Δt is time interval (s) for each scan of the PLC program; k is ratio of heat capacities of the gas mixture at constant pressure and at constant volume (i.e. Cp/Cv, assumed to be 1.28 for CO_2 and 1.4 for N_2), and η is compressor/pump efficiency (70% assumed). The absolute energy is normally divided by the amount of CO_2 in the product stream to obtain the specific energy.

From Fig. 6, it can be deduced that at purity of 95% considered to be the requirement for CCS, product recoveries from 52 to 55% and 78 to 83% for 8 kPa and 5 kPa respectively can be obtained, considering predicted and experimental results. There is a large drop in recovery in increasing desorption pressure from 5 to 8 kPa. The CO_2 isotherm on 13x is steeper (indicating stronger adsorption) in the lower pressure region. Hence, very low evacuation pressures would ideally be required to assist in the effective removal of the adsorbed components and regeneration of the adsorbent for the next operation. This explains the modest recoveries realized at the selected evacuation pressures (with regeneration based on only pressure reduction). For a given purity, the simulation model (in Aspen Adsorption) gave a slightly higher CO_2 recovery. This could be due to differences and variations in the product tank pressure and flow velocity of the rinse gas from the product tank to the bed compared to fixed values used in the simulations.

Table 4-Summarized performance results of experimental runs

	Total feed time (s)	Des P (kPa)	Purity $\%CO_2$	Recovery $\%CO_2$	Sp. Energy $MJ/kgCO_2$	Productivity $kgCO_2/kg.ads/hr$
Run 1	40	8	88.04	75.65	0.35	0.12
Run 2	60	8	90.9	70.44	0.34	0.1
Run 3	80	8	92.38	64.05	0.33	0.08
Run 4	100	8	93.54	58.47	0.33	0.07
Run 5	120	8	95.85	51.27	0.31	0.08
Run 6	40	5	89.2	88.01	0.33	0.12
Run 7	60	5	91.2	82.57	0.31	0.11
Run 8	80	5	92.80	80.83	0.33	0.13
Run 9	100	5	95.83	75.32	0.33	0.11
Run 10	120	5	96.68	73.77	0.32	0.09

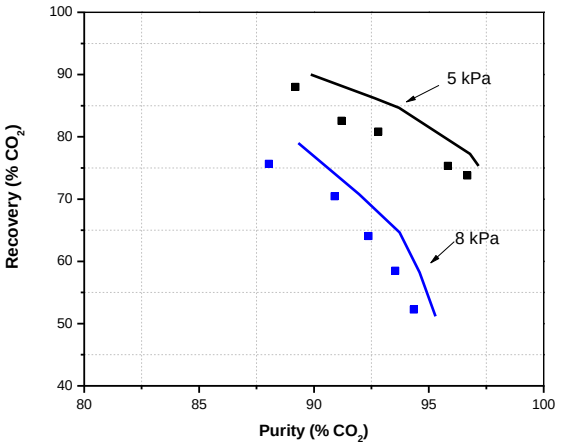

Fig. 6-Purity- recovery characteristic for desorption at 5- and 8- kPa. Dot =experiment; line = simulation.

Plots of product purity versus specific power and productivity are also given in Fig. 7 for the experimental runs at vacuum pressures of 5 and 8 kPa. It is generally difficult to achieve very high CO_2 product purity at the higher desorption pressure of 8 kPa. As purity is extended beyond 90% (by means of increasing adsorption time to allow more CO_2 adsorption), productivity drops drastically even though similar specific power consumption is realized in comparison with the operation at the lower (deeper) evacuation pressure of 5 kPa. The performance of the VSA system is heavily reliant on the vacuum level reached at the end of desorption [19]. It directly affects all the performance criteria evaluated. From Fig. 6, both purity and recovery of CO_2 are higher at 5 kPa than 8 kPa. CO_2 product recovery rate depends on adsorbent working capacity, which generally increases with decreasing vacuum pressure. The vacuum pressure also affects specific power consumption. The specific power consumption depends on the amount of CO_2 recovered and the compression ratio in the equation (Eq. 4) used to calculate the power consumption. Generally, higher vacuum pressure leads to reduced compression ratio, but lower product purity and recovery, while deeper vacuum pressure leads to higher compression ratio, but increased product purity and recovery.

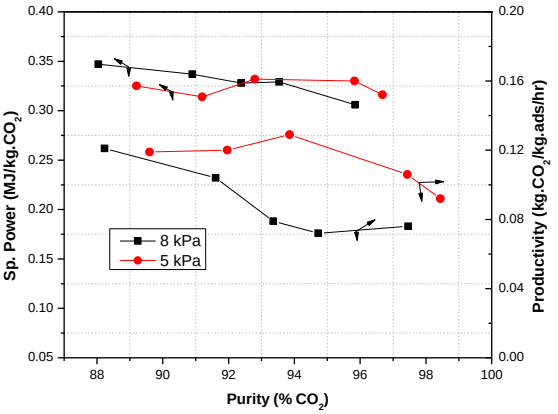

Fig. 7-Specific power, product purity, and productivity at 5- and 8- kPa vacuum pressure (experimental results)

Therefore, the specific power consumption at a given vacuum pressure may be higher or lower depending on which of the two factors- amount of CO_2 product gas recovered and compression ratio, has the dominant effect. Similar specific power consumption values were obtained for 5 and 8 kPa desorption. This means the increase of compression ratio in 5 kPa is compensated for by the increase in CO_2 productivity.

Productivity (kg CO_2/kg ads/hr) relates directly to adsorbent working capacity (which depends on desorption pressure) and inversely to cycle time. At a higher vacuum pressure, shorter cycle time is required in order to avoid more CO_2 loss in the effluent as breakthrough time is shorter; however, working capacity reduces as more of the adsorbed components will not be recovered. Thus, similar to specific power consumption, productivity at a given vacuum pressure can be higher or lower depending on which factor dominates. For a given purity, productivity was higher for 5 kPa desorption than 8 kPa. Thus, even though shorter cycle time is required by 8 kPa to yield comparable recovery (e.g. compare runs 1 and 9 in Table 4), the less amount of gas processed overrides the shorter cycle time.

4.3. Effect of Adsorption Step Time

The amount of feed gas introduced into the bed during adsorption is also an important factor affecting the process performance. With the feed flowrate fixed, the total amount of feed is determined by the feed time. It can be seen from Fig. 8 that CO_2 recovery declined while purity increased with feeding time at each given desorption pressure. This is due to the larger breakthrough of CO_2 in the feed effluent with longer adsorption step times. Fig. 9a shows that the CO_2 concentration front moves up the column with each increase in adsorption step time from 40 to 120 seconds, leading to increase in CO_2 concentration in the effluent (z/L = 1) from 0.04 to 0.142. Also with the longer adsorption time, more CO_2 will be adsorbed; some co-adsorbed N_2 is even displaced by the CO_2 in the incoming feed hence, the bed is more enriched in CO_2 (see Fig. 9b) and this explains the increase in purity. Interestingly, due to the product rinse, purity was not affected as much as recovery with changes in adsorption step time and even changes in evacuation pressure. Thus, the usual penalty (in terms of purity) for increasing recovery by reducing adsorption time is not large in the current case. Taking desorption at 8 kPa for example, purity ranged between 88 and 96%, while recovery ranged from 52 to 76% CO_2. Comparable product purities were obtained at the evacuation pressures examined, but 8 kPa desorption yielded lower recovery compared with desorption at 5 kPa, with the recovery (at 8 kPa) decreasing rapidly with increase in adsorption step time. Cyclic breakthrough time is shortened at higher evacuation pressure as more CO_2 remains in the bed at the end of desorption. Therefore, more CO_2 is lost in the effluent with increase in adsorption time, which accounts for the relatively lower recovery rate at 8 kPa.

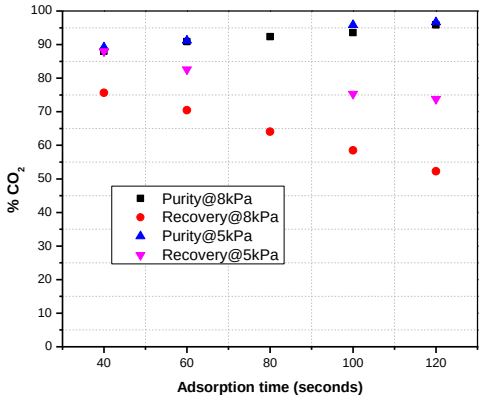

Fig. 8-Product purity and recovery as a function of adsorption step time for desorption at 5- and 8- kPa (experimental results)

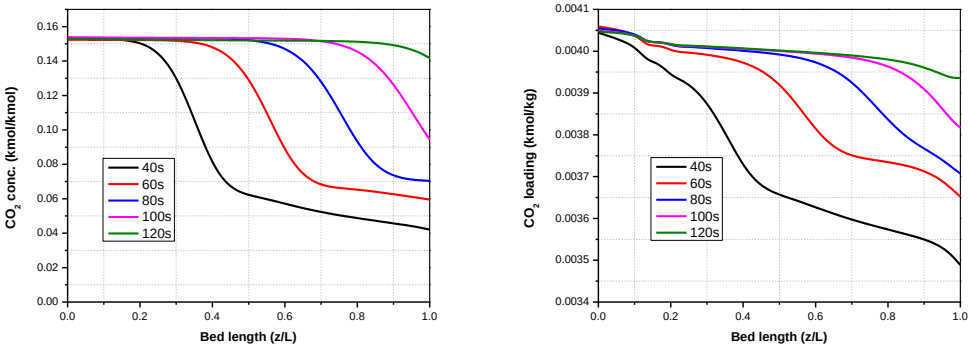

Fig. 9- Concentration profiles of CO_2 as function of bed length during adsorption for a desorption pressure of 8 kPa (a) Gas-phase concentration, kmol/kmol (b) Solid-phase concentration (kmol/kg)

4.4. Roles of Product Rinse and Pressure Equalisation Steps

The roles played by the product rinse and associated pressure equalization steps can further be explained using the column profiles of pressure, temperature and concentration. Generally, the state of the bed (pressure, temperature and concentration) at the commencement of the desorption step (which recovers the product gas) determines the performance of the process [5]. The pressure reached in the column after the first PE step differs slightly with desorption pressure and adsorption step time, and thus, affects the amount of product gas used to rinse the bed (as shown in Fig. 10). Overall, only about 20 - 25% of the product gas is recycled to the bed during the rinse step and the value increases with lower desorption pressure due to the lower pressure reached during the preceding PE step. At shorter adsorption time, less amount of CO_2 is produced and hence, the ratio of CO_2 in the rinsing gas to CO_2 in the product is higher even though the starting pressure is higher. The purge ratio decreases to a minimum and rises as adsorption time further increases due to the decrease in column pressure, which provides room for more rinse gas to be admitted to the bed.

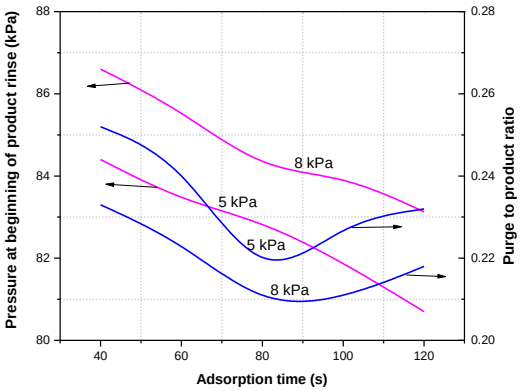

Fig. 10 Bed pressure at the commencement of product rinse and ratio of purge gas to product at different adsorption step times.

5. Conclusions

A new VSA cycle sequence has been proposed for CO2 capture aimed at a high product purity and lower specific power consumption. A four-bed PSA/VSA rig packed with zeolite 13x adsorbent was used to test the cycle performance. Results from experimental runs were compared with predicted results from the commercial Aspen adsorption software and good agreements was obtained. 64% of CO_2 can be recovered with 92.4% purity from feed gas containing 15% CO_2 at a desorption pressure of 8 kPa, while 5 kPa desorption can produce >75% recovery with a higher purity of >95%CO_2 and specific power consumption of ~ 0.33 MJ/kgCO_2. The efficiency of the VSA process strongly depends on the vacuum pressure, and many reported studies are based on the use of very low vacuum pressures. Thus, the performance realized in the current study using a relatively higher vacuum pressure level of 8 kPa is indicative of the effectiveness of the proposed process cycle. The study shows that even though many cycle configurations have already been tested, new cycle configurations can still be developed to give improved performance.

Acknowledgements

The authors gratefully acknowledge the funding provided by the Australian Government through its CRC Program to support this CO2CRC research project.

References

[1] Boot-Handford ME, Abanades JC, Anthony EJ, Blunt MJ, Brandani S, Mac Dowell N, et al. Carbon capture and storage update. Energy Environ Sci 2014;7:130–89.
[2] Rackley SA. Carbon capture and storage. Burlingto, MA: Butterworth-Heinemann; 2010.
[3] Ebner AD, Ritter JA. State-of-the-art adsorption and membrane separation processes for carbon dioxide production from carbon dioxide emitting industries. Sep Sci Technol 2009;44:1273–421.
[4] Agarwal A, Biegler LT, Zitney SE. A superstructure-based optimal synthesis of PSA cycles for post-combustion CO2 capture. AIChE J 2010;56:1813–28.
[5] Ling J, Ntiamoah A, Xiao P, Webley PA, Zhai Y. Effects of feed gas concentration, temperature and process parameters on vacuum swing adsorption performance for CO2 capture. Chem Eng J 2015;265:47–57.
[6] Shen C, Yu J, Li P, Grande CA, Rodrigues AE. Capture of CO2 from flue gas by vacuum pressure swing adsorption using activated carbon beads. Adsorption 2011;17:179–88.

[7] Haghpanah R, Nilam R, Rajendran A, Farooq S, Karimi IA. Cycle synthesis and optimization of a VSA process for postcombustion CO2 capture. AIChE J 2013;59:4735–48.
[8] Krishnamurthy S, Rao VR, Guntuka S, Sharratt P, Haghpanah R, Rajendran A, et al. CO2 capture from dry flue gas by vacuum swing adsorption: A pilot plant study. AIChE J 2014;60:1830–42.
[9] Reynolds SP, Mehrotra A, Ebner AD, Ritter JA. Heavy reflux PSA cycles for CO2 recovery from flue gas: Part I. Performance evaluation. Adsorption 2008;14:399–413.
[10] Xiao P, Zhang J, Webley P, Li G, Singh R, Todd R. Capture of CO2 from flue gas streams with zeolite 13X by vacuum-pressure swing adsorption. Adsorption 2008;14:575–82.
[11] Kikkinides ES, Yang RT, Cho SH. Concentration and recovery of CO2 from flue gas by pressure swing adsorption. Ind Eng Chem Res 1993;32:2714–20.
[12] Zhang J, Webley PA. Cycle development and design for CO2 capture from flue gas by vacuum swing adsorption. Environ Sci Technol 2008;42:563–9.
[13] Warmuzinski K. Effect of pressure equalization on power requirements in PSA systems. Chem Eng Sci 2002;57:1475–8.
[14] Chen Y. Carbon dioxide recovery from low concentration sources. US8137435 B2, 2012.
[15] Wang L, Yang Y, Shen W, Kong X, Li P, Yu J, et al. Experimental evaluation of adsorption technology for CO2 capture from flue gas in an existing coal-fired power plant. Chem Eng Sci 2013;101:615–9.
[16] Delgado JA, Uguina MA, Sotelo JL, Águeda VI, Sanz A, Gómez P. Numerical analysis of CO2 concentration and recovery from flue gas by a novel vacuum swing adsorption cycle. Comput Chem Eng 2011;35:1010–9.
[17] Chaffee AL, Knowles GP, Liang Z, Zhang J, Xiao P, Webley PA. CO2 capture by adsorption: Materials and process development. Int J Greenh Gas Control 2007;1:11–8.
[18] Li G, Xiao P, Webley P, Zhang J, Singh R, Marshall M. Capture of CO2 from high humidity flue gas by vacuum swing adsorption with zeolite 13X. Adsorption 2008;14:415–22.
[19] Webley PA. Adsorption technology for CO2 separation and capture: a perspective. Adsorption 2014;20:225–31.
[20] Wang L, Liu Z, Li P, Wang J, Yu J. CO2 capture from flue gas by two successive VPSA units using 13XAPG. Adsorption 2012;18:445–59.
[21] Chue KT, Kim JN, Yoo YJ, Cho SH, Yang RT. Comparison of activated carbon and zeolite 13X for CO2 recovery from flue gas by pressure swing adsorption. Ind Eng Chem Res 1995;34:591–8.
[22] Maring BJ, Webley PA. A new simplified pressure/vacuum swing adsorption model for rapid adsorbent screening for CO2 capture applications. Int J Greenh Gas Control 2013;15:16–31.
[23] Ling, J., Ntiamoah, A. Xiao, Penny., Webley, Paul A. Zhai, Yuchun. The Sensitivity of CO2 Capture by Vacuum Swing Ad. Ind. Eng. Chem.Res. 2015 in review.
[24] Sircar S. Basic Research Needs for Design of Adsorptive Gas Separation Processes. Ind Eng Chem Res 2006;45:5435–48.
[25] Ruthven DM, Farooq S, Knaebel KS. Pressure Swing Adsorption. VCH Publishers Inc., New York; 1994.
[26] Liu Z, Wang L, Kong X, Li P, Yu J, Rodrigues AE. Onsite CO2 Capture from Flue Gas by an Adsorption Process in a Coal-Fired Power Plant. Ind Eng Chem Res 2012;51:7355–63.
[27] Ritter JA, Bhadra SJ, Ebner AD. On the use of the dual-process Langmuir model for correlating unary equilibria and predicting mixed-gas adsorption equilibria. Langmuir 2011;27:4700–12.
[28] Lin L-C, Berger AH, Martin RL, Kim J, Swisher JA, Jariwala K, et al. In silico screening of carbon-capture materials. Nat Mater 2012;11:633–41.